Comparing the Power Losses of Power Supplies for Fast-Field Cycling Nuclear Magnetic Resonance Equipment

Marco Lima[1], Bruno Pereira[1], Duarte M. Sousa[2], António Roque[3] and Elmano Margato[3]

[1] Department of Electrical and Computer Engineering
Instituto Superior Técnico – Universidade de Lisboa, Lisboa (Portugal)
marco.lima@tecnico.ulisboa.pt, bruno.i.pereira@tecnico.ulisboa.pt

[2] Department of Electrical and Computer Engineering
Instituto Superior Técnico & INESC-ID – Universidade de Lisboa, Lisboa (Portugal)
duarte.sousa@tecnico.ulisboa.pt

[3] Department of Electrical Engineering
ESTSetúbal - Instituto Politécnico de Setúbal & INESC-ID, Setúbal (Portugal)
antonio.roque@estsetubal.ips.pt

[4] Centro de Electrotecnia e Electrónica Industrial
ISEL &INESC-ID, Lisboa (Portugal)
efmargato@isel.ipl.pt

Abstract. The main feature of the Fast-Field Cycling (FFC) Nuclear Magnetic Resonance (NMR) power supplies is to drive a controlled current fulfilling the requirements of this technique. This feature allows fast switching the current of the FFC magnet and performing accurate and repetitive current cycles. When designing this equipment the power losses is not a fundamental parameter of the optimization process but are estimated in order to validate the topology of the final solution giving that the efficiency of the power solution influences the power consumption, and therefore the operational costs, which should be minimized.
Under this context, from the power efficiency viewpoint, the power losses of two possible solutions are compared and discussed in this paper. Typical FFC current cycles are used as reference in order to balance the pros and cons of both solutions.

Key words

Power supply; Power losses; Fast-Field Cycling; DC-DC conversion.

1. Introduction

Fast-Field Cycling (FFC) Nuclear Magnetic Resonance (NMR) power supplies integrate a complex apparatus, which is composed by the following main blocks [1]-[5]:

- Power supply;
- Magnet;
- Signal acquisition system;
- RF circuit/Excitation system;
- Computer;
- Probe head and sample holder.

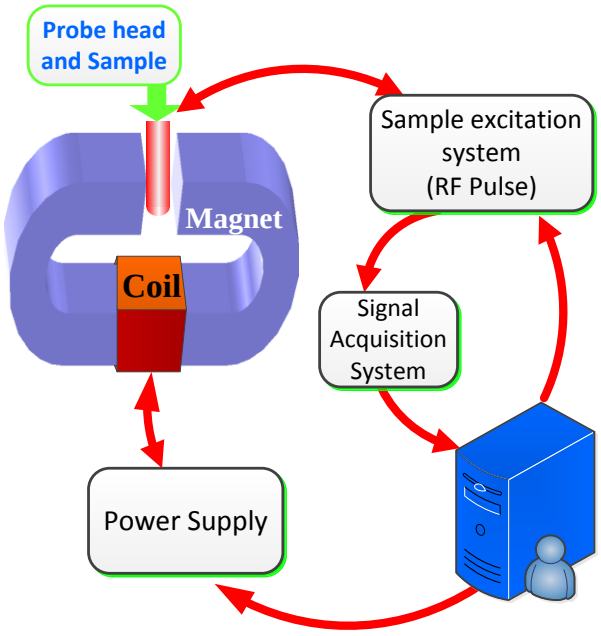

Fig. 1. Main parts of a FFC-NMR equipment

The topology and performance of these power supplies depend strongly on the electrical parameters of the FFC-NMR magnet. For other hand, the requirements of this experimental technique have been fulfilled taking advantage of the power electronics devices and topologies [5]-[11].

Comparisons between FFC-NMR solutions are generically done considering the magnetic field range

and the dynamics obtained when cycling the magnetic flux density or the magnet current [12]-[18]. In the present case, two solutions supplying the same magnet are compared based on their power losses. The described solutions cover a flux density range corresponding to a magnet current range from 0 to 10A.

2. Electric Circuits

The comparison between the two power supplies will be done based on the power losses and power consumption during typical magnet current cycles. Both solutions should present similar dynamics, i.e., should be able to control the magnet current from 0 to 10A and the magnet current transients should occur within the milliseconds range.

A. Solution A

The global circuit of the Solution A is represented in Fig. 2.

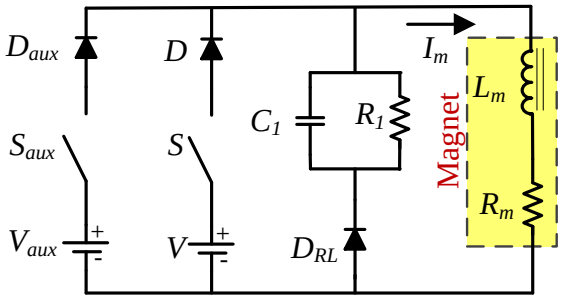

Fig. 2. Global circuit of the *Solution A*

The *Solution A* is constituted by two voltage sources (V and V_{aux}), diodes (D, D_{aux} and D_{RL}), switches (IGBTs S and S_{aux}) and a RC filter (C_1 and R_1), being R_m and L_m the resistance and self-inductance of the magnet, respectively.

The *Solution A* operation principle depends on the state of the switches (S and S_{aux}), being typical to define 3 operation modes: Up, Steady-state and Down.

A.1 - Up mode

During the Up mode the switch S_{aux} is "ON" and the switch S is "OFF", corresponding to the equivalent circuit represented in Fig. 3. Neglecting the diodes drop voltage, the electrical equation corresponding to the Up mode is:

$$V_{aux} \approx \gamma_{aux}(1-\gamma)\left(L_m \frac{di_m}{dt} + R_m i_m\right) \quad (1)$$

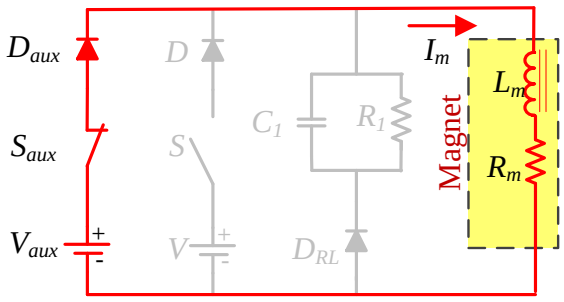

Fig. 3. Equivalent circuit for the Up mode – Solution A

A.2 - Steady-state mode

During the steady-state mode the switch S is under an "ON/OFF" control and the switch S_{aux} is "OFF", corresponding to the equivalent circuit represented in Fig. 4. The electrical equation corresponding to the Steady-state mode (neglecting the diodes drop voltage) is:

$$V \approx \gamma(1-\gamma_{aux})\left(L_m \frac{di_m}{dt} + R_m i_m\right) \quad (2)$$

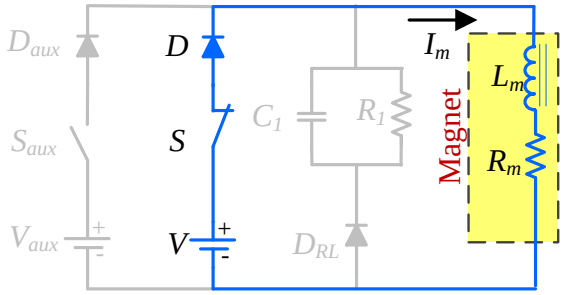

Fig. 4. Equivalent circuit for the Steady-state mode – Solution A

A.3 - Down mode

During the Down mode the switches S and S_{aux} are "OFF", corresponding to the equivalent circuit represented in Fig. 5. Neglecting the diodes drop voltage, the electrical equation corresponding to the Down mode is:

$$\frac{1}{C}\int i_m dt \approx (1-\gamma-\gamma_{aux})\left(L_m \frac{di_m}{dt} + R_m i_m\right) \quad (3)$$

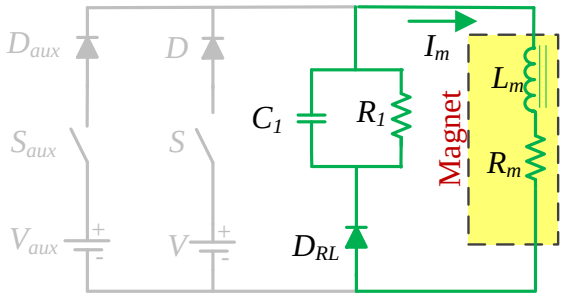

Fig. 5. Equivalent circuit for the Down mode – Solution A

The states of the switches for each operation mode are summarized in Table I.

TABLE I. – States of the switches – Solution A

	Solution A		
	Up	**Steady-state**	**Down**
γ_1	0	1	0
γ_{aux}	1	0	0

It should be referred that to avoid short-circuits between the voltage source V and the auxiliary voltage source V_{aux} a dead time is considered between the sequences "OFF–ON" of the switches S and S_{aux}.

B. Solution B

The global circuit of the *Solution A* is represented in Fig. 6.

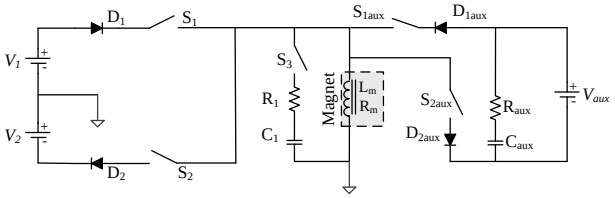

Fig. 6. Global circuit of the *Solution B*

Solution B owns 5 switches ((IGBTs S_1, S_2, S_3, S_{1aux}, S_{2aux}), 4 diodes (D_1, D_2, D_{1aux}, D_{2aux}) and 3 voltage sources (V_1, V_2, V_{aux}). It includes also 2 RC filters (R_1C_1 and $R_{aux}C_{aux}$). The magnet used to analyze this circuit is the same of *Solution A* (R_m, L_m).

For *Solution B*, the magnet current is controlled in order to set the magnet current control under the following operation modes: Up, Steady-state, Down and Compensation.

B.1 - Up mode

During the Up mode the switch $S1_{aux}$ is "ON" and the other switches are "OFF", corresponding to the equivalent circuit represented in Fig. 6. Neglecting the diodes drop voltage, the electrical equation corresponding to the Up mode is:

$$V_{aux} \approx \gamma_{1aux}(1-\gamma_{2aux})(1-\gamma_1-\gamma_2-\gamma_3)\left(L_m\frac{di_m}{dt}+R_m i_m\right) \quad (4)$$

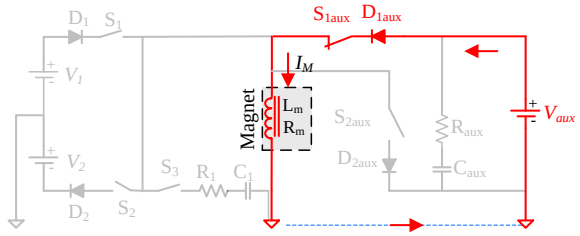

Fig. 6. Equivalent circuit for the Up mode – Solution B

B.2 - Steady-state mode:

During the steady-state mode the switches S_1 and S_3 are under an "ON/OFF" control and the other switches are "OFF", corresponding to the equivalent circuit represented in Fig. 7. The electrical equation corresponding to the Steady-state mode (neglecting the diodes drop voltage) is:

$$\gamma_1\bar{\gamma}_3 V_1 \approx (1-\gamma_1-\gamma_{1aux}-\gamma_{2aux})\left(L_m\frac{di_m}{dt}+R_m i_m\right) \quad (5)$$

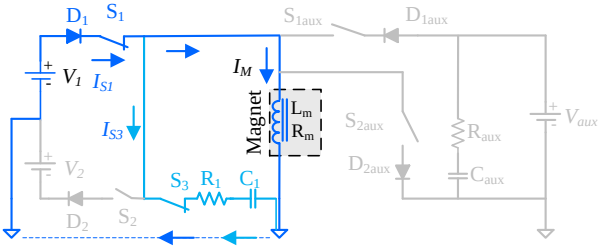

Fig. 7. Equivalent circuit for the Steady-state mode – Solution B

B.3 - Down mode

During the Down mode the switches S_3 and S_{2aux} are "ON" according to the instaneous voltage drop of the magnet and the other switches are "OFF, corresponding to the equivalent circuit represented in Fig. 8. Neglecting the diodes drop voltage, the electrical equation corresponding to the Down mode is:

$$L_m\frac{di_m}{dt}+R_m i_m \approx \gamma_3\overline{\gamma_{2aux}}\frac{1}{C_1}\int i_m dt \approx -\gamma_{2aux}\bar{\gamma}_3\frac{1}{C_{aux}}\int i_m dt \quad (6)$$

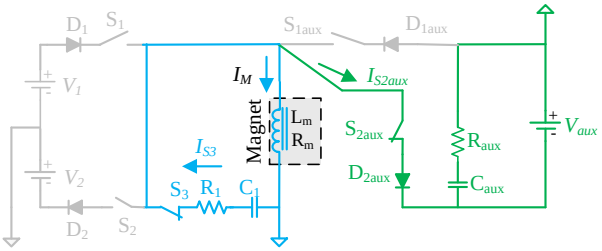

Fig. 8. Equivalent circuit for the Down mode – Solution B

B.4 - Compensation mode:

The Compensation mode is set for low current values of the magnet. This procedure is mandatory in order to eliminate the effect of the Earth magnetic field, memory effect of the magnetic circuits and parasitic currents. During the Compensation mode, it is typical to invert the magnet current, being the load current driven by the voltage source V_2. In this case, the switch S_2 is "ON" and the other switches are "OFF, corresponding to the equivalent circuit represented in Fig. 9.

Neglecting the diodes drop voltage, the electrical equation corresponding to the Compensation mode is:

$$-V_2 \approx \gamma_2(1-\gamma_1-\gamma_3)\left(L_m\frac{di_m}{dt}+R_m i_m\right) \quad (6)$$

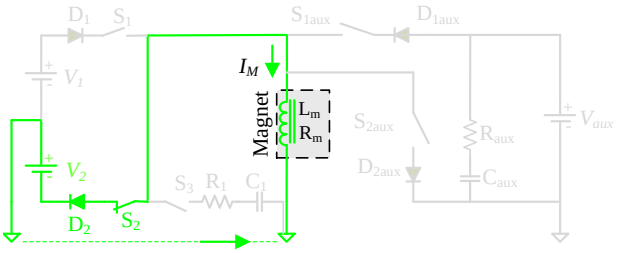

Fig. 9. Equivalent circuit for the Compensation mode – Solution B

The states of the switches for the *Solution B* operation modes are summarized in Table II.

TABLE II. – States of the switches – Solution B

	Solution B		
	Up	**Steady-state**	**Down**
γ_1	0	1	0
γ_2	0	0	0
γ_3	0	1	1
γ_{1aux}	1	0	0
γ_{2aux}	1	0	0

3. Joule and switches losses

To compare the power consumption and power losses of *Solution A* and *Solution B*, two typical current cycles, with the characteristics shown in Fig. 10, are used.

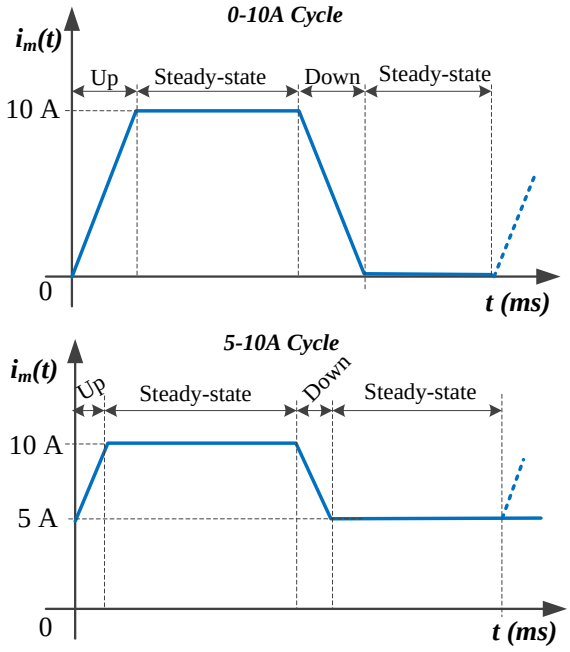

Fig. 10. Typical current cycles

As first approach, the power losses are due to the switches losses (switching losses and conduction losses of the switches) and the Joule losses of the magnet. The power losses along a typical current cycle, change as represented in Fig. 11.

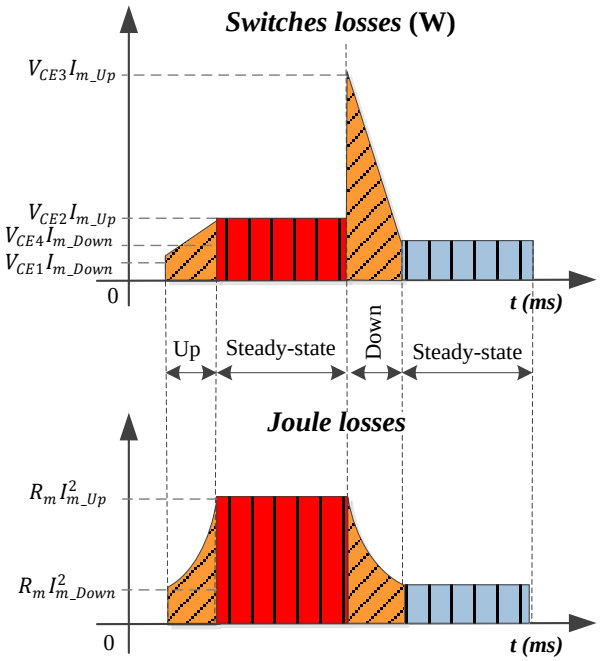

Fig. 11. Power losses along a current cycle (V_{CE} – voltage drop of the switches; i_{m_Up} – steady-state magnet current during the Up mode; i_{m_Down} – steady-state magnet current during the Down mode)

A. Solution A

Solution A was analysed considering the two typical cycles represented in Fig. 10 with the characteristics summarized in Table III.

TABLE III. – Current cycle characteristics – Solution A

CYCLE	0-10A	5-10A
Period of the cycle [ms]	100	100
Δt [ms] – Up mode	3.2	1.8
Δt [ms] – Steady-state mode – 10A	46.8	48.2
Δt [ms] – Down mode	3.5	1.8
Δt [ms] – Steady-state mode – 0A	46.5	48.2
Δi_m [A] (i_{m_Up} - i_{m_Down})	10	5
VCE1 [V]	2.2	2.2
VCE2 [V]	19.3	19.3
VCE3 [V]	786.4	786.4
VCE4 [V]	50	34.3
V[V]	50	50
V_{aux} [V]	400	400
R_m [Ω]	3	
L_m [mH]	270	

The power losses and the power supplied for both cycles are represented in Fig. 12 and Fig. 13.

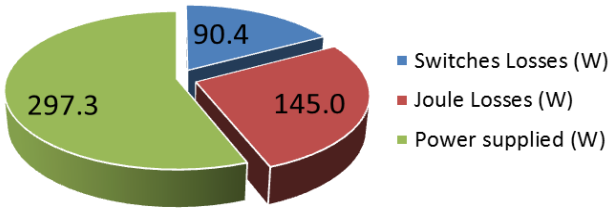

Fig. 12. Power losses and power supplied along the 0-10A cycle – Solution A

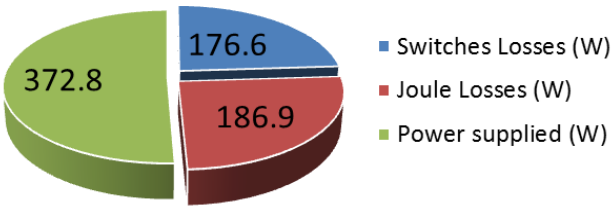

Fig. 13. Power losses and power supplied along the 5-10A cycle – Solution A

B. Solution B

Solution B was analysed considering the two typical cycles represented in Fig. 10 with the characteristics summarized in Table IV.

TABLE IV. – Current cycle characteristics – Solution B

CYCLE	0-10A	5-10A
Period of the cycle [ms]	100	100
Δt [ms] – Up mode	3.2	1.8
Δt [ms] – Steady-state mode – 10A	46.8	48.2
Δt [ms] – Down mode	3.5	1.8
Δt [ms] – Steady-state mode – 0A	46.5	48.2
Δi_m [A] (i_{m_Up} - i_{m_Down})	10	5
VCE1 [V]	2.2	2.2
VCE2 [V]	1.3	1.3
VCE3 [V]	786.4	786.4
VCE4 [V]	32	16.3
$V_1 = V_2$ [V]	32	32
V_{aux} [V]	400	400
R_m [Ω]	3	
L_m [mH]	270	

For *Solution B*, the power losses and the power supplied for both cycles are represented in Fig. 14 and Fig. 15.

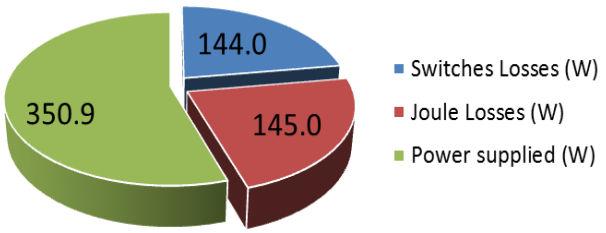

Fig. 14. Power losses and power supplied along the 0-10A cycle – Solution B

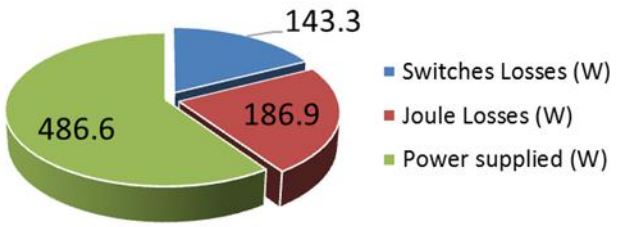

Fig. 15. Power losses and power supplied along the 5-10A cycle – Solution B

4. Conclusion

The solutions presented in this paper are analysed considering the specifications and requirements of the FFC-NMR technique.

Comparing the power losses and power consumption for both solutions, it should be referred that under similar conditions:

- the Joule losses, the switches losses and the power consumption are similar for *Solutions A and B*;
- *Solution A* is simpler considering the number of semiconductors/switches required and the complexity of the control system;
- concerning the requirements of the FFC-NMR technique, *Solution B* includes features, as for instance the compensation of the Earth magnetic field or parasitic currents, which are difficult to achieve with *Solution A*.

Considering the factors above, it is clear that *Solution B* presents advantages. Anyway, depending on the characteristics of the FFC magnet, *Solution A* can be adopted constituting an adequate solution not only from the technical point of view since from the economical viewpoint is a less expensive option.

Acknowledgement

This work was supported by national funds through Instituto Politécnico de Setúbal, for the support to the paper presentation and *FCT – Fundação para a Ciência e a Tecnologia*, under project UID/CEC/50021/2013.

References

[1] F. Noack, "NMR Field-Cycling Spectroscopy: Principles and Applications," Prog. NMR Spectrosc., vol. 18, pp. 171-276, 1986.

[2] R. Seitter, R. O. Kimmich, "Magnetic Resonance: Relaxometers," Encyclopedia of Spectroscopy and Spectrometry, Academic Press, London, pp. 2000-2008, 1999.

[3] E. Anoardo, G. Galli, G. Ferrante, "Fast-Field-Cycling NMR: Applications and Instrumentation," Applied Magnetic Resonance, vol. 20, pp. 365-404, 2001.

[4] R. Kimmich and E. Anoardo, “Field-Cycling NMR relaxometry,” Progress in NMR Spectroscopy, 44, pp. 257-320, 2004.

[5] Pine KJ, Davies GR, Lurie DJ, “Field-cycling NMR relaxometry with spatial selection”, Magn Reson Med, 63(6), 2010, pp. 1698-702.

[6] J. Constantin, J. Zajicek, F. Brown, “Fast Field-Cycling Nuclear Magnetic Resonance Spectrometer,” Rev. Sci. Instrum., vol. 67, pp. 2113-2122, 1996.

[7] D. M. Sousa, E. Rommel, J. Santana, J. Fernando Silva, P. J. Sebastião, A. C. Ribeiro, “Power Supply for a Fast Field Cycling NMR Spectrometer Using IGBTs Operating in the Active Zone,” 7th European Conference on Power Electronics and Applications (EPE1997) , Trondheim, Norway, pp. 2.285-2.290, 1997.

[8] D. M. Sousa, G. D. Marques, J. M. Cascais, P. J. Sebastião “Desktop Fast-Field Cycling Nuclear Magnetic Resonance Relaxometer”, Solid State Nuclear Magnetic Resonance, Vol. 38, 2010, pp. 36-43.

[9] A. Roque, S. F. Pinto, J. Santana, Duarte M. Sousa, E. Margato, J. Maia, “Dynamic Behavior of Two Power Supplies for FFC NMR Relaxometers,” IEEE International Conference on Industrial Technology – ICIT 2012, Athens - Greece, 2012.

[10] D. M. Sousa, P. A. L. Fernandes, G. D. Marques, A. C. Ribeiro, P. J. Sebastião, “Novel Pulsed Switched Power Supply for a Fast Field Cycling NMR Spectrometer,” Solid State Nuclear Magnetic Resonance, Vol. 25, 2004, pp. 160-166.

[11] Rou-Yong Duan, Bo-Han Chen, and Rong-Jong Wa, “Design of High-Efficiency Dual-Input Interleaved DC-DC Converter,” IEEE, International Conference on Industrial Technology (ICIT), 2014.

[12] Nathaniel I. Matter, Greig C. Scott, Thomas Grafendorfer, Albert Macovski, Steven M. Conolly, “Rapid polarizing field cycling in magnetic resonance imaging”, IEEE Trans Med Imaging, 25(1), 2006, pp. 84-93.

[13] F. Bonetto and E. Anoardo, “Proton field-cycling nuclear magnetic resonance relaxometry in the smectic A mesophase of thermotropic cyanobiphenyls: Effects of sonication”, Journal of Chemical Physics, Vol.121, 2004.

[14] P. James Ross, Lionel M. Broche, and David J. Lurie, “Rapid Field-Cycling MRI Using Fast Spin-Echo”, Magnetic Resonance in Medicine vol. 73, 2015, pp. 1120–1124.

[15] David J. Lurie and al, “Fast field-cycling magnetic resonance imaging - Imagerie de resonance magnétique en champ cyclé, Multiscale NMR and relaxation/RMN et relaxation multi-échelles,” C. R. Physique, 11, 2010, pp. 136–148.

[16] D.J. Lurie, G.R. Davies, M.A. Foster, J.M.S. Hutchison, “Field-cycled PEDRI imaging of free radicals with detection at 450 mT,” Magnetic Resonance Imaging, Vol. 23, 2005, pp. 175–181.

[17] K M Gilbert and all, “Design of field-cycled magnetic resonance systems for small animal imaging,” Phys. Med. Biol., Vol.51, 2006, pp. 2825–2841.

[18] Patrick N. Morgan, Steven M. Conolly and Albert Macovski, “Resistive Homogeneous MRI Magnet Design by Matrix Subset Selection”, Magnetic Resonance in Medicine, vol. 41, 1999, pp.1221–1229.